

Supersoftening of transverse phonons in $Zr_{41}Ti_{14}Cu_{12.5}Ni_{10}Be_{22.5}$ bulk metallic glass

Wei Hua Wang,* Hai Yang Bai, J. L. Luo, Ru Ju Wang, and D. Jin

Institute of Physics & Center for Condensed Matter Physics, Chinese Academy of Sciences, 100080 Beijing, China

(Received 20 December 1999)

Acoustic properties and low-temperature specific heat of $Zr_{41}Ti_{14}Cu_{12.5}Ni_{10}Be_{22.5}$ alloy in glassy, fully crystallized and equilibrium crystalline states have been investigated. It is found that a large amount of free volume is quenched in the bulk metallic glass (BMG) which is obtained at a low-cooling rate, even fully crystallization cannot remove all the free volume from the alloy. A supersoftening of long-wavelength transverse acoustic phonons in the BMG relative to its equilibrium crystalline state is observed. The origins for the phenomenon are discussed. The finding has significance for understanding of the glassy state as well as the excellent glass forming ability of the glass forming alloy.

Metallic glasses have long represented an intriguing class of materials. For many years, however, a very high-cooling rate ($>10^5$ K/s) necessary to prevent crystallization, limits specimen geometry to be very thin ribbons or wires (~ 10 – 100 m thick), making the measurements of many physical properties difficult.^{1,2} The key features of the microstructure and physical properties as well as their relationship are still poorly understood. The recent discovery of a new family of bulk metallic glasses (BMG)^{3,4} offers opportunities for understanding the metallic glassy state and investigating the physical properties by using various physical methods. Ultrasonic measurement provides a powerful tool for studying the structure of matter; the larger geometry of the BMG's is very suitable for acoustic measurement.⁵ The differences between glassy and crystalline states in acoustic feature and long-wavelength phonons have significance for the understanding of the unique microstructural characteristics and physical properties of the BMG. In this paper, we present the results of acoustic and low-temperature specific-heat experiments on a representative $Zr_{41}Ti_{14}Cu_{12.5}Ni_{10}Be_{22.5}$ BMG with excellent glass forming ability and properties.³ A supersoftening of long-wavelength transverse-acoustic phonons in the BMG relative to its equilibrium crystalline states is observed; the phenomenon is not simply attributed to the density difference between the two states. The results have significance for our exploring the reasons for the excellent glass forming ability of the alloy as well as our understanding of the glassy metallic state.

$Zr_{41}Ti_{14}Cu_{12.5}Ni_{10}Be_{22.5}$ ingots were prepared by inductive levitation melted under a Ti-gettered Ar atmosphere. The ingots were remelted together in a silica tube and quenched in water to get cylindrical rod with 15-mm diameter (the cooling rate is estimated to be about 10 K/s). The details of the preparation procedure can be referred to in Refs. 5 and 6. Amorphous nature as well as homogeneity of the BMG was ascertained by x-ray diffraction (XRD), differential scanning calorimeter (DSC), transmission electron microscopy (TEM) and small-angle neutron scattering SANS.^{5,6} The fully crystallized $Zr_{41}Ti_{14}Cu_{12.5}Ni_{10}Be_{22.5}$ alloy was prepared by annealing the BMG at 773 K in vacuum for more than 4 h. The annealing temperature is far larger than the crystallization temperature T_x (712 K).^{5,6} XRD and DSC results as well as TEM observations confirm that the

BMG was fully crystallized. The equilibrium crystalline phase of $Zr_{41}Ti_{14}Cu_{12.5}Ni_{10}Be_{22.5}$ alloy rod with 15 mm in diameter was prepared by remelting the ingots in a silica tube and solidified at a cooling rate of 0.03 K/s XRD verifies the fully crystalline state that has also been confirmed by DSC result; no heat release DSC peaks, which indicate the crystallization of an amorphous phase, have been observed. These alloy rods were machined down to 10 mm in diameter and cut to a length of about 10 mm. By grinding off the outer surface, any possible oxide materials from the quartz tube container were removed, and the identical composition of the three alloys was ascertained by careful chemical analysis. The ends of the cylinder were carefully polished flat and parallel. The prepared specimens were used for density, acoustic velocities, and specific-heat measurements. All these measurements were two and three times repeatedly performed using cylinders from different sections of the alloy rods. The acoustic velocities of the alloys were measured at room temperature by using a pulse echo overlap method.⁷ The excitation and detection of the ultrasonic pulses were provided by X or Y cut (for longitudinal and transverse waves, respectively) 10-MHz quartz transducers. The transducers were bonded to one end of the specimen. The ultrasonic wave are excited by the transducer, reflected from the opposite end of the rod, and detected by the same transducer. The effects due to bonding material between the transducer and the sample was neglected as the typical thickness of the

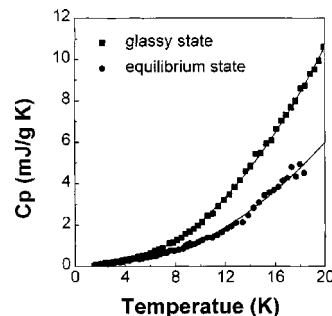


FIG. 1. Specific heat of the $Zr_{41}Ti_{14}Cu_{12.5}Ni_{10}Be_{22.5}$ alloys in glassy and equilibrium crystalline states. The solid lines are fits of the data from 10 to 18 K, since $\theta_D(T)$ for a metallic glass and crystalline exhibits a strong temperature dependence below 8 K.

TABLE I. A comparison of the properties of the metallic glasses state (Y_a) and fine-grained crystallized state (Y_c) of the $Zr_{41}Ti_{14}Cu_{12.5}Ni_{10}Be_{22.5}$ alloy.

Alloy	ρ (g/cm ³)	v_l (km/s)	v_s (km/s)	K (GPa)	G (GPa)	$\theta_D^A(T)$ (K)	T_m (K)
Glassy state	6.125	5.174	2.472	114.1	37.41	326.8	945
Crystallized state	6.192	5.446	2.807	118.6	48.8	370.9	1109
$(Y_c - Y_a)/Y_a$ (%)	1.1	5.2	13.5	3.9	30.3	13.4	17.3

band was lower than 4 μm . The travel time of ultrasonic waves propagating through the sample with a 10 MHz carry frequency was measured using a MATEC 6600 ultrasonic system with a measuring sensitive of 0.5 ns. The elastic constants, e.g., bulk modulus K and shear modulus G , are derived from the acoustic velocities using the well-known relations.^{7,8} In calculating the Debye temperature θ_D we treat the alloy as a monatomic lattice with an average cellular volume; θ_D can be represented as follows⁹

$$\theta_D(\text{elastic}) = \frac{h}{k_B} \left(\frac{9}{4\pi\Omega_0} \right)^{1/3} \left(\frac{1}{\nu_l^3} + \frac{2}{\nu_s^3} \right)^{-1/3}, \quad (1)$$

where h and k_B are Planck and Boltzman constants respectively, Ω_0 is the atomic volume, and ν_l , and ν_s are longitudinal and transverse ultrasonic velocities, respectively. The values of elastic constants and θ_D of the BMG calculated from ultrasonic data are in good agreement with the results measured by other methods.^{3,8} Low-temperature specific heats were measured in an adiabatic calorimeter between 1.8 and 20 K using a standard discontinuous heating method.⁹ Density ρ was measured by the Archimedian principle and the accuracy was evaluated to be 0.005 g/cm³.

Figure 1 presents temperature-dependent specific heat C_p of the BMG and equilibrium crystalline alloy from 1.8 to 18 K. It can be clearly seen that the temperature dependent C_p is markedly different for the two states; the glassy state has larger specific heat than that of the crystalline state. The C_p is analyzed by fitting to it a polynomial form $C_p = \gamma T + \beta T^3$ using a least-squares procedure,

$$\beta(T) = \frac{12\pi^4 R}{5} \left(\frac{1}{\theta_D(T)} \right)^3 \quad (\text{Ref. 10}),$$

where R is the gas constant. The effective Debye temperature $\theta_D(T)$ can be calculated from the fit. Since $\theta_D(T)$ for metallic glass and crystalline alloy exhibits a strong temperature dependence below 8 K, the data over the limited temperature range 10 to 20 K were fitted. Table I shows the agreement

obtained for the Debye temperature calculated from the calorimetric $\theta_D^L(T)$ and acoustic $\theta_D^A(T)$ data. From Eq. (1), we get $\theta_D^A(T) \approx \text{const } \rho^{1/3} \nu_s$,

$$\frac{\Delta\theta}{\theta} \approx \frac{1}{3} \frac{\Delta\rho}{\rho} + \frac{\Delta\nu_s}{\nu_s} \approx 38.7\%,$$

which is in good agreement with experimental results. Following the free-electron model, γ is related to the density-of-state at the Fermi level $N(E_F)$ by $\gamma = (1/3)\pi^2 k_B^2 N(E_F)$. Accordingly, the estimated $N(E_F)$ values are 4.7 eV (unit cell)⁻¹ and 2.8 eV (unit cell)⁻¹ for glassy and equilibrium states, respectively. The BMG has larger $N(E_F)$ value as compared to its corresponding crystalline state.

The values for the ρ , ν_l , ν_s , as well as the elastic and thermal parameters for the alloys in glassy and crystallized states are listed in Table I. Large changes in the ν_s (13.5%), θ_D (13.4%), and G (30.3%) and small changes in the ρ (1.1%), ν_l (5.2%), and K (3.9%) between the two states can be seen in Table I. The results indicate the softening of the transverse elastic modulus (i.e., the softening of the long-wavelength transverse phonons) in the BMG relative to its crystallized state. Elastic softening is a common feature for the most amorphization processes usually accompanied by a $\sim 25\%$ decrease in the average velocity of sound, which corresponds to a $\sim 50\%$ decrease in the average of G .¹¹ The softening in the BMG is consistent with that of amorphization process. Table II contrasts the remarkable large changes in the ν_s (39.7%), θ_D (38.7%), and G (102%) and small changes in ρ (3.6%), ν_l (7.7%), and K (-15.8%) between the glassy and equilibrium crystalline states. The results indicate that an extremely large softening exists between the two states. The decrease in G is substantially larger than the typical 10%–50% reported for alloys that undergo an order-disorder transformation below melting temperature.^{11,12} It is even larger than the G softening observed for many metals during heating to melting.¹³ Since the results between the calorimetric and acoustic measurements agree, this indicates that the softening of the transverse mode may be extended to low temperature. XRD results¹⁴ show that the crystallized

TABLE II. A comparison of the properties of the metallic glassy state (Y_a) and equilibrium crystalline state (Y_e) of the $Zr_{41}Ti_{14}Cu_{12.5}Ni_{10}Be_{22.5}$ alloy.

Alloy	ρ (g/cm ³)	v_l (km/s)	v_s (km/s)	K (GPa)	G (GPa)	$\theta_D^L(T)$ (K)	$\theta_D^A(T)$ (K)	T_m (K)
Glassy state	6.125	5.174	2.472	114.1	37.41	324.1	326.8	945
Equilibrium state	6.346	5.571	3.454	96.0	75.7	435.0	453.2	1527
$(Y_e - Y_a)/Y_a$ (%)	3.6	7.7	39.7	-15.8	102.0	34.3	38.7	61.6

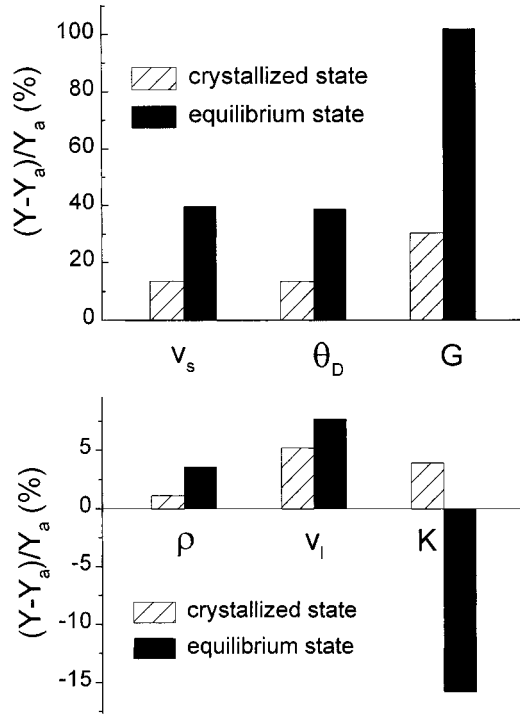


FIG. 2. A comparison of the relative changes of the parameters of the crystallized and equilibrium states compared to amorphous state. (Y_a), the properties of metallic glasses state; Y , the properties of the crystalline state.

and equilibrium crystalline alloys contain different crystalline phases. Due to the complex of the multicomponents and the Be element, the crystalline phases cannot be identified so far.³ However, the crystallized alloy has much more crystalline peaks indicating more distinct crystalline phases compared with the equilibrium alloy. The possible multiphase mixture, which causes an amount of defects, e.g., interfaces, would lead to a looser structure and a little softening of G compared with an equilibrium alloy consisting of only a single phase. Figure 2 contrasts the relative change of the ρ , v_s , θ_D , and G of the crystallized and equilibrium states compared with the glassy state. The parameters especially for the v_s , G , and θ_D of the equilibrium state have much larger relative changes than those of the crystallized state. The ρ change (3.6%) means that high density of free volume is quenched in the BMG, even if it is obtained with a slow cooling rate. Even full crystallization, which causes 1.1% ρ change, can only partially remove the free volume. The conclusion that the BMG contains a large amount of free volume has been confirmed by high-pressure experiments,¹⁵ which shows the BMG has a larger volume change upon pressure compared with crystalline solids, because the free volume can be removed through the structural relaxation induced by high pressure. Positron annihilation studies¹⁶ also confirm that excess volume in the order of 0.1% is quenched in the BMG at cooling rates as low as 1–2 K/s. The supersoftening phenomenon is confirmed by the low-melting temperature, T_m of the BMG ($T_m=945$ K) compared to that of its equilibrium state ($T_m=1527$ K) as shown in Table II. The T_m of the BMG is 582 K lower. T_m is related to θ_D and critical static mean-square displacement, $\langle\mu^2\rangle$ as:¹¹ $T_m = (Mk_B\theta_D^2)/9h^2\langle\mu^2\rangle$, where M is the average atomic mass.

The supersoftening results in the larger decrease of the T_m of the glassy state. So, compared with the equilibrium crystalline state, the BMG has three characteristics: (1) the BMG contains high-density free volume even if it has more random packed microstructure compared with conventional metallic glasses, fully crystallization can only remove part of the free volume; (2) the BMG has higher $N(E_F)$, and lower T_m ; (3) the BMG has a super softened transverse phonons mode relative to its equilibrium state. The characteristics are similar to the melting of a solid, in that a very high density of point defects combined with a softened phonon mode leads to melting.¹⁷

Shear modulus of all solids depend on the interatomic distance or molar volume and especially the repulsive branch of the interatomic potential,¹⁸ the quenched-in free volume changes the density of the BMG, and definitely leads to the softening of the shear modulus. Theoretically, simulations prove that a large softening of transverse phonons in an oxide glass is attributed to gross density change;¹⁹ the reduced of G is from the change of the local atomic density in the looser structure of the glasses. The oxide glasses exhibit a large decrease in acoustic velocity relative to the crystal, this is attributed to the large density change, e.g., for vitreous SiO_2 , $\Delta\rho/\rho \approx 20\%$.²⁰ However, the BMG has denser packed microstructure compared with conventional metallic glasses and oxide glasses.²¹ The ρ change is much smaller than that of the oxide glasses. Such an enormous net change in the G cannot be mainly attributed to the ρ difference between the glassy and crystalline states. Lam *et al.*¹¹ point out that the softening of G associates with static atomic displacement $\langle\mu\rangle$ and anharmonic vibration in a metallic glass. Our other work shows that the BMG possess a larger anharmonicity,²² however, the supersoftening cannot be mainly related to the anharmonicity either, because the effect of the static atomic displacement on the softening is nearly twice as large as that of anharmonic vibration; the static atomic displacement is a general measure of the chemical and topological disorder and hence can be used as a general disorder parameter for characterizing a glassy solid.¹¹ Miglio *et al.*²³ also found that the larger atomic mean-square displacement gave rise to a lower elastic energy. Figure 3 contrasts the differences of the G and v_s upon $\langle\mu^2\rangle$ estimated from the generalized Lindemann melting criterion;¹¹ it can be clearly seen that the alloy with smaller G and v_s has larger $\langle\mu^2\rangle$, indicating that the increased magnitude of $\langle\mu^2\rangle$ compared to its equilibrium state leads to the lower frequencies of a transverse phonon.¹⁹ There is an intrinsic reason for the high disorder of the structure, that results in the supersoftening of the transverse phonons in the BMG. The non-Coulomb part of the interatomic potential is large due to the overlap of closed electron shells for transition metals in the highly dense and randomly packed BMG, a marked effect of the configuration of the outer electron on the elastic constant, especially G , has been pointed out by Koster;²⁴ the high density of the electronic state at the Fermi level is also likely to soften the band strength.²³ The connection between the static atomic disorder, larger anharmonicity, the high density of electronic states at the Fermi level and supersoftening of shear modulus presents evidence that there are other intrinsic softening of transverse phonons in the BMG. Because all the factors have close relation with the microstructure, we infer that the su-

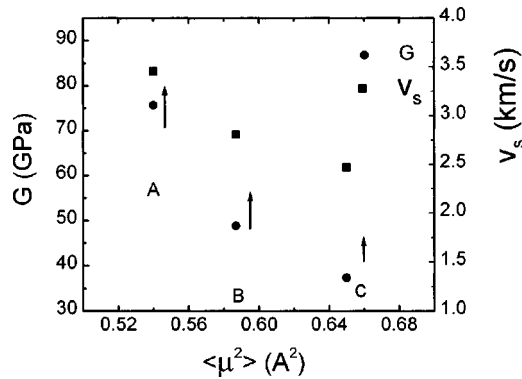


FIG. 3. The contrast of the G and v_s on the critical static mean-square atomic displacement, $\langle \mu^2 \rangle$ of the three states is estimated from the generalized Lindeman melting criterion Ref. 11. A, B, and C in the figure indicate the equilibrium, crystallized and glassy states, respectively). The alloy with smaller G and v_s , has larger $\langle \mu^2 \rangle$, indicating that the increased magnitude of $\langle \mu^2 \rangle$ compared to its equilibrium state, leads to lower frequencies of transverse phonon in the BMG.

persoftening of the transverse phonon is mainly attributed to the unique microstructural characteristics of the glassy state. The supersoftening confirms highly static atomic disorder microstructure in the BMG.

The finding of the supersoftening also provides a support to the recent studies on the atomic diffusion in the BMG, which suggests a highly cooperative diffusion mechanism involving many atoms, which differs from that of its ordered counterpart.^{25–27} It is suggested^{28,29} that if the basic diffusion mechanism involves the collective motion of a large number of atoms, a far smaller frequency (typically 10^{10} s^{-1}) is expected to be several orders of magnitude lower than the De-

bye frequency (about 10^{12} to 10^{13} s^{-1}). The measurements of the low-frequency vibration (softening of long-wave phonons) means many atoms move cooperatively.²⁹ There is a strong consistency between the highly-collective diffusion and our observation; one could think of the quenched-in free volume in the BMG as intrinsic soft spots where cooperative atomic hopping processes can take place. The finding of the supersoftening also has significance for our understanding the excellent glass forming ability of the BMG, which can be obtained with a critical cooling rate less than 1 K/s .⁵ The supersoftening confirms that marked differences exist in the electronic state; atomic interaction and static atomic disorder between the glassy and equilibrium crystalline states, and the microstructure of the BMG, can be regarded as closer to that of the liquid state. The liquidlike highly random packed structure and cooperative atomic diffusion mechanism of the BMG strongly inhibit the nucleation and growth in the supercooled liquid state, and result in excellent glass forming ability.

In conclusion, we find that the $\text{Zr}_{41}\text{Ti}_{14}\text{Cu}_{12.5}\text{Ni}_{10}\text{Be}_{22.5}$ BMG is of a super softening of long-wavelength transverse-acoustic phonons combining an amount of free volume relative to its equilibrium crystalline state. The supersoftening is not simply attributed to the small density difference between the amorphous and crystalline states; it is rather mainly related to the unique microstructural characteristics of the metallic glassy state. The supersoftening may have close relation with the excellent glass forming ability of the glass forming system.

The authors are grateful to the financial support of the National Natural Science Foundation of China (Grant Nos. 59871059, 59925101, and 19874075) and the Chinese National Microgravity Laboratory of CAS.

*Author to whom correspondence should be addressed. Electronic address: whw@aphy.iphy.ac.cn

¹W. Klement, R. H. Willens, and P. Duwez, *Nature* (London) **187**, 869 (1960).

²A. L. Greer, *Science* **267**, 1947 (1995).

³W. L. Johnson, *Mater. Sci. Forum* **225–227**, 35 (1996); R. D. Conner *et al.*, *Acta Mater.* **46**, 6089 (1998).

⁴A. Inoue, *Mater. Trans., JIM* **36**, 866 (1995).

⁵W. H. Wang and R. J. Wang, *Appl. Phys. Lett.* **74**, 1083 (1999).

⁶W. H. Wang, Q. Wei, and H. Y. Bai, *Appl. Phys. Lett.* **71**, 58 (1997).

⁷D. Schreiber, *Elastic Constants and Their Measurement* (McGraw-Hill, New York, 1973).

⁸R. Truell *et al.*, *Ultrasonic Methods in Solid State Physics* (Academic, New York, 1969), p. 10.

⁹H. Y. Bai *et al.*, *J. Appl. Phys.* **79**, 361 (1996).

¹⁰P. Debye, *Ann. Phys. (Leipzig)* **39**, 789 (1912).

¹¹N. Q. Lam *et al.*, *MRS Bull.* **19**, 41 (1994).

¹²L. E. Rehn *et al.*, *Phys. Rev. Lett.* **59**, 2987 (1987).

¹³J. L. Tallon, *J. Phys. Chem. Solids* **41**, 837 (1984).

¹⁴W. H. Wang (unpublished).

¹⁵W. H. Wang and Z. X. Bao, *Phys. Rev. B* **61**, 3166 (2000).

¹⁶C. Nagel, *et al.*, *Phys. Rev. B* **57**, 10 224 (1998).

¹⁷R. W. Cahn, *Nature* (London) **400**, 512 (1999).

¹⁸C. Kittel, *Introduction to Solid State Physics* (Wiley, New York, 1971).

¹⁹D. Weaier, *et al.*, *Acta Metall.* **19**, 779 (1971).

²⁰O. L. Anderson, in *Physical Acoustics*, edited by W. P. Mason (Academic, New York, 1965), Vol. III B.

²¹W. H. Wang, Q. Wei, and S. Friedrich, *Phys. Rev. B* **57**, 8211 (1998).

²²W. H. Wang and R. J. Wang (unpublished).

²³L. Miglio, *et al.*, *Appl. Phys. Lett.* **74**, 3654 (1999).

²⁴K. Koester, *Metall. Rev.* **6**, 1 (1961).

²⁵H. Ehmle, A. Heesemann, K. Raetzke, F. Faupel, and U. Geyer, *Phys. Rev. Lett.* **80**, 4919 (1998).

²⁶X. P. Tang *et al.*, *Phys. Rev. Lett.* **81**, 5358 (1998).

²⁷S. K. Sharma and F. Faupel, *J. Mater. Res.* **14**, 3200 (1999).

²⁸E. C. Stelter and D. Lazarus, *Phys. Rev. B* **36**, 9545 (1987).

²⁹H. R. Schober, *Physica A* **201**, 14 (1993).